

# Formulation of the Lagrangian particle model LAPMOD and its evaluation against Kincaid SF<sub>6</sub> and SO<sub>2</sub> datasets



Roberto Bellasio<sup>a,\*</sup>, Roberto Bianconi<sup>a</sup>, Sonia Mosca<sup>a</sup>, Paolo Zannetti<sup>b</sup>

<sup>a</sup> Enviroware srl, Via Dante 142, 20863 Concorezzo, MB, Italy

<sup>b</sup> The EnviroComp Institute, 500 Stone Pine Road, #3038, Half Moon Bay, CA 94019, USA

## HIGHLIGHTS

- The theory behind a new Lagrangian particle model (LAPMOD) is described.
- Directly coupled with CALMET, meteorological processor of the US-EPA CALPUFF model.
- Coupled to AERMET output files through its LAPMET processor.
- Detailed accounting of peak-to-mean concentration fluctuations, for odor modeling.
- Evaluated against Kincaid SO<sub>2</sub> and SF<sub>6</sub> field experiments with good results.

## ARTICLE INFO

### Article history:

Received 16 March 2017

Received in revised form

17 May 2017

Accepted 22 May 2017

Available online 25 May 2017

### Keywords:

Lagrangian particle model

Kernel smoother

Model evaluation

Kincaid

## ABSTRACT

This paper presents the Lagrangian particle model LAPMOD for modeling time-variable emissions in atmosphere of inert and radioactive gases and aerosols. LAPMOD is fully interfaced with the meteorological model CALMET (Scire et al., 1999a), part of the US-EPA recommended CALPUFF modeling system (EPA, 2017), and can also use the meteorological input files produced with the AERMET meteorological processor of US-EPA recommended model AERMOD (EPA, 2004).

The paper outlines the theory on which LAPMOD is based and provides the results of the evaluation of LAPMOD against the Kincaid SF<sub>6</sub> and SO<sub>2</sub> classical field studies and tracer experiments. The performance of LAPMOD is successfully evaluated with the Model Evaluation Kit (Olesen, 2005) and compared with that of other air quality models.

© 2017 Elsevier Ltd. All rights reserved.

## 1. Introduction

In the last decades, Lagrangian particle dispersion models (LPDMs) have become more appealing as modeling tools to simulate the atmospheric dispersion of pollutants thanks to their ability to reproduce the stochastic nature of turbulence (e.g. Thomson and Wilson, 2012). Lagrangian particle models simulate pollutant releases by following a number of independent computational particles – each one representing a fraction of the released mass - in a sequence of finite time intervals. The motion of each particle is driven by a time-varying velocity field, which can be divided into an average component, the average wind, plus a fluctuation velocity describing the effects of atmospheric turbulence and those wind variations not included in the mean component. The fluctuation

velocity can be described by a non-linear form of the Langevin stochastic differential equation.

While particles in Lagrangian particle models are generally considered computational markers of the atmospheric fluid that allow the reconstruction of the concentration field of the pollutant at later times, the description of released matter in terms of particles allows easy incorporation of some physical processes the pollutant may undergo, including radioactive decay and deposition. Since particles can represent the pollutants as gas or aerosol, deposition and gravitational settling can also be taken into account.

The advantages of Lagrangian particle models with respect to Eulerian models and analytical models are described for example in Zannetti (1990).

LPDMs are widely used tools in the field of atmospheric pollution studies. For example, they are used to estimate the emission rates of specific sources starting from monitored concentrations (e.g. Park et al., 2016) and to simulate atmospheric dispersion over

\* Corresponding author.

E-mail address: [rbellasio@enviroware.com](mailto:rbellasio@enviroware.com) (R. Bellasio).

complex terrain (e.g. Rakesh et al., 2015). LPDMs can be coupled with CFD in a relatively simple way, therefore they are used to evaluate the dispersion of pollutants within complex urban environments due to accidental hazardous releases (e.g. Hanna et al., 2011; Armand et al., 2014). They can be used on different spatial scales to simulate different kinds of releases (e.g. Bellasio et al., 2012; Brioude et al., 2013; Hegarty et al., 2013).

Lagrangian particle models often require a large number of particles to obtain statistically sound results and short time steps to integrate the equation of motion of the particles. However, the computational resources commonly available nowadays make them suitable for implementations oriented both to real-time applications, and to simulate long periods.

This paper introduces the Lagrangian particle model LAPMOD.

The development of LAPMOD began more than 20 years ago. During the years the model had different names, but its core remained the same. The development started from the model developed by Zannetti (1990) and one of the first modified version was the model described by Bianconi et al. (1999). After some years a photochemical module was inserted in the model, as described in Zanini et al. (2002), but this research direction was abandoned and the model was re-transformed into a tool for inert pollutants. With the aim to speed up the simulations, the algorithm for calculating the concentrations starting from particle positions and masses was substituted from the brute-force counting method to the use of kernels (Vitali et al., 2006). During the last decade the model has been further tested and modified, for example adding the description of aerosols and their granulometric distributions, the dry and wet deposition algorithms, the radioactive decay of isotopes (both in air and in deposited material), two numerical plume rise methods and the algorithm for managing odor pollution, as described in the following paragraphs. Moreover, a source-attribution algorithm has been recently added to the model (Bonafe' et al., 2015). The model has been adopted by some Italian Agencies, as for example the Regional Agency for the Environment of Region Emilia Romagna (ARPA-ER), and the National Institute for Environmental Protection and Research (ISPRA).

LAPMOD is fully coupled to the diagnostic meteorological model CALMET (Scire et al., 1999a), preprocessor of the US-EPA preferred/recommended dispersion model CALPUFF (Scire et al., 1999b; EPA, 2017). LAPMOD, through its preprocessor LAPMET, can also use as an alternative the meteorological input files of the US-EPA preferred dispersion model AERMOD (EPA, 2004). LAPMOD can describe several types of sources: point, linear, volume, and area (circles, rectangles and irregular polygons) that can arbitrarily vary with time. Point sources may also be buoyant due to thermal or mechanical effects, and the stack-tip downwash and partial plume penetration effects are included. LAPMOD also reduces the run time by making use of a kernel smoother for the calculation of the concentration field.

The paper first describes the theory behind the model and its design. Then the results of its evaluation against the classical Kincaid SF<sub>6</sub> and SO<sub>2</sub> datasets (Hanna and Paine, 1989; Olesen, 2005) are presented, including a comparison with the performance of other widely used models.

## 2. Model formulation

This section contains a detailed description of the LAPMOD formulation. The first part illustrates how each particle is moved according to a mean wind component and a random turbulent velocity fluctuation. Then the coefficients needed to determine the turbulent fluctuations along the horizontal and vertical directions and under different stability conditions are presented.

### 2.1. Particles movement

According to the Lagrangian approach, the description of the atmospheric dispersion of a pollutant is obtained by computing a number of possible different trajectories that air masses at the same time in the same position may follow due to the stochastic nature of turbulence. The mass of the emitted species is then fractioned among some particles acting as markers. These portions of atmospheric fluids are macroscopic since they include a large number of molecules, but they are small enough to be considered as points. The movement of the particles is due to the effect of the mean wind field and the turbulent diffusion that is supposed to act on particles through an additional stochastic wind velocity component.

The random walk induced by turbulence is assumed to be first-order Markovian. Given the position of a particle at time  $t$  (s), its position at the time  $t+\Delta t$  (s) is given by:

$$x_i(t + \Delta t) = x_i(t) + \Delta t(u_i + u'_i)$$

where  $i = 1, 2, 3$  indicates respectively the  $x$ ,  $y$  and  $z$  direction,  $u_i$  is the mean wind component along the  $i$ -th direction ( $m\ s^{-1}$ ) and  $u'_i$  represents the turbulent velocity fluctuation along the same  $i$ -th direction ( $m\ s^{-1}$ ). The time evolution of the velocity fluctuation is described in the most general terms by the non-linear Langevin equation introduced by Thomson (1987):

$$du'_i = a_i(x, u'_i, t)dt + b_{ij}(x, u'_i, t)d\xi_j(t)$$

where  $a_i$  ( $m\ s^{-2}$ ) and  $b_{ij}$  ( $m\ s^{-1.5}$ ) are functions of space, velocity and time, and  $d\xi_j(t)$  ( $s^{-0.5}$ ) is a random increment of a Wiener process with independent components, each with zero mean and variance equal to  $dt$ .

Both  $a_i$  and  $b_{ij}$  coefficients are linked to the structure of turbulence through functional relations with the meteorological variables. Many schemes have been investigated in literature for describing these deterministic coefficients. The  $a_i$  acceleration coefficients are implemented in LAPMOD as a quadratic function of the velocity (Franzese et al., 1999):

$$a_i = \alpha u_i^2 + \beta u_i + \gamma$$

The  $\alpha$  ( $m^{-1}$ ),  $\beta$  ( $s^{-1}$ ) and  $\gamma$  ( $m\ s^{-2}$ ) coefficients vary depending on the turbulence conditions that are discriminated according to the ratio  $L/z_i$ , where  $L$  is the Monin–Obukhov length (m) and  $z_i$  is the mixing layer height (m).

### 2.2. Coefficients for vertical component under unstable conditions

The coefficients  $\alpha$ ,  $\beta$  and  $\gamma$  for the vertical component under unstable conditions ( $L/z_i < -1$ ) are those proposed by Franzese et al. (1999):

$$\alpha(z) = \frac{\frac{1}{3}GW_4 - \frac{1}{2}\frac{W_3}{W_2}(GW_3 - C_0\varepsilon) - W_2GW_2}{W_4 - \frac{W_3^2}{W_2} - W_2^2}$$

$$\beta(z) = \frac{GW_3 - 2\alpha W_3 - C_0\varepsilon}{2W_2}$$

$$\gamma(z) = GW_2 - \alpha W_2$$

where  $C_0$  is the adimensional Kolmogorov constant (the suggested value is 3 according to Du (1997), but this value can be changed when running LAPMOD),  $\varepsilon$  is the eddy dissipation rate ( $m^2\ s^{-3}$ ),  $W_n$  indicates the  $n$ -th order moment of the distribution of the vertical

fluctuation velocities  $w(z)$  and  $GW_n$  is the corresponding gradient along the vertical. The above equations show that the acceleration is completely defined if the first four moments of the velocity are known.

Following [Franzese et al. \(1999\)](#), these analytical expressions for the second and the third moments are used:

$$\frac{W_2}{w_*^2} = a_1 + a_2 \left(\frac{z}{z_i}\right)^{\frac{2}{3}} \left(1 - \frac{z}{z_i}\right)^{\frac{4}{3}}$$

$$\frac{W_3}{w_*^3} = a_3 \left(\frac{z}{z_i}\right) \left(1 - \frac{z}{z_i}\right)^2$$

where  $z_i$  is the convective boundary layer height (m),  $w_*$  is the convective scale velocity ( $m\ s^{-1}$ ), and the three adimensional coefficients are  $a_1 = 0.05$ ,  $a_2 = 1.7$  and  $a_3 = 1.1$ .

The fourth moment is calculated as ([Hibberd and Sawford, 1994](#)):

$$W_4 = 3.5W_2^2$$

and the eddy dissipation rate is given by ([Luhar and Britter, 1989](#); [Weil, 1990](#)):

$$\epsilon = 0.4 \frac{w_*^3}{z_i}$$

In LAPMOD the derivatives that appear in the equations for  $\alpha$ ,  $\beta$  and  $\gamma$  are obtained by analytically deriving the expressions for the moments.

The motion is uncorrelated along the three components, i.e.  $b_{ij} = 0$  for  $i \neq j$ . The  $b$  coefficient for the vertical component for unstable conditions is given by:

$$b = \sqrt{C_0 \epsilon}$$

### 2.3. Coefficients for vertical component under neutral and stable conditions

For neutral and stable conditions ( $L/z_i \geq -1$ ), the coefficients  $\alpha$ ,  $\beta$  and  $\gamma$  for the vertical component of the  $\alpha$  coefficient are set to match the equation proposed first by [Wilson et al. \(1983\)](#) for inhomogeneous Gaussian turbulence:

$$\alpha(z) = \frac{GW_2^2}{2W_2^2} = \frac{GW_2}{W_2}$$

$$\beta = -\frac{1}{T_L}$$

$$\gamma(z) = W_2 GW_2$$

where  $T_L$  is the Lagrangian time scale (s).

### 2.4. Coefficients for horizontal components

The  $a_i$  coefficient for the horizontal component, for any stability condition, is given by:

$$a_i = -\frac{u'_i}{T_{Li}}$$

For neutral and stable conditions ( $L/z_i \geq -1$ ) and for the

horizontal component under any stability the  $b$  coefficient is given by:

$$b = W_2 \sqrt{\frac{2}{T_L}}$$

### 2.5. Lagrangian time scales and velocity fluctuations

Lagrangian time scales and velocity fluctuations depend on the stability conditions. In LAPMOD they are calculated as described by [Hanna et al. \(1982\)](#), except where indicated in the following.

Under unstable conditions ([Hurley and Physik, 1993](#)):

$$T_{LU} = T_{LV} = 0.15 \frac{z_i}{\sigma_v}$$

$$T_{LW} = 0.6 \frac{z_i}{w_*}$$

and  $\sigma_v$  ( $m\ s^{-1}$ ) is given by:

$$\sigma_v = u_* \left(12 - 0.5 \frac{z_i}{L}\right)^{\frac{1}{3}}$$

Under neutral conditions:

$$\sigma_u = 2u_* \exp\left(-\frac{3fz}{u_*}\right)$$

$$\sigma_v = \sigma_w = 1.3u_* \exp\left(-\frac{2fz}{u_*}\right)$$

$$T_{LU} = T_{LV} = T_{LW} = \frac{0.5z}{\sigma_w \left(1 + 15 \frac{fz}{u_*}\right)}$$

where  $f$  ( $s^{-1}$ ) is the Coriolis parameter,  $z$  is the height above ground (m) and  $u_*$  is the friction velocity ( $m\ s^{-1}$ ).

Under stable conditions:

$$\sigma_u = 2u_* \left(1 - \frac{z}{z_i}\right)$$

$$\sigma_v = \sigma_w = 1.3u_* \left(1 - \frac{z}{z_i}\right)$$

$$T_{LU} = 0.15 \frac{z_i}{\sigma_u} \sqrt{\frac{z}{z_i}}$$

$$T_{LV} = 0.07 \frac{z_i}{\sigma_v} \sqrt{\frac{z}{z_i}}$$

$$T_{LW} = 0.10 \frac{z_i}{\sigma_w} \left(\frac{z}{z_i}\right)^{0.8}$$

Above the mixing height, the velocity fluctuations along the three components follow the Langevin equation for homogeneous conditions and turbulence is strongly attenuated.

A particle can get above the boundary layer due to its motion or because the boundary layer drops. Whenever a particle gets above the boundary layer the vertical component of its fluctuation velocity is set to 0. Then the particle moves according to the Langevin

equation for homogeneous conditions with the coefficients for horizontal components calculated with  $T_L = 1000$  s and  $\sigma = 0.01$  m s<sup>-1</sup>.

The Langevin equation for each component is integrated forward in time with a constant time step equal to 0.15 s (Wilson and Zhuang, 1989), except for convective conditions where a variable time step is applied and calculated according to Thomson (1987).

## 2.6. Sources, plume rise, and deposition

LAPMOD can simulate emission scenarios with multiple point, line, area, and volume sources with arbitrarily-varying (down to 1 s) emission rates of different pollutants.

Pollutants can be inert or radioactive-decaying, in the form of gases or aerosols. Aerosol size distribution is log-normal, with AMAD (Aerodynamic Mean Aerosol Diameter) and GSD (Geometrical Standard Deviation) that depend on the substance. The log normal continuous distribution is represented as a discrete distribution in the model and for each aerosol particle emitted there are several computational particles generated, each of them with a diameter assigned with probability consistent with the size distribution.

Point sources can be buoyant, and plume rise can be simulated numerically using Webster and Thomson (2002) or Janicke and Janicke (2001) algorithms. The two algorithms are similar, but the second one contains equations of conservation of water mass and is therefore more suitable for wet plumes, such as those emitted by scrubbers in desulfuration processes (Presotto et al., 2005). The equations of the plume rise models are numerically integrated by a fourth-order Runge–Kutta method implemented within LAPMOD. The plume-induced turbulence is described as in Webster and Thomson (2002). LAPMOD also includes an algorithm for the stack tip downwash and can take into account the partial plume mixing height penetration as described by Manins (1979).

In LAPMOD, the particles affected by the plume rise follow the trajectory of a bending plume until the plume loses its buoyancy. Afterwards, these particles move like any other non-buoyant particle, driven by the local average wind velocity plus the turbulent components simulated by the Langevin equation described above.

LAPMOD includes algorithms for dry deposition of gases, and dry and wet depositions for aerosols. Wet deposition of gases is not implemented yet, however it is generally neglected because most gases are relatively insoluble (e.g. Webster and Thomson, 2014). The dry deposition is calculated by the resistance analogy method (e.g. Seinfeld and Pandis, 1998), while the settling velocity of aerosols is calculated as described by Zhang et al. (2001). The wet deposition of aerosols is calculated as described by Baklanov and Sorensen (2001). The mass of each computational particle may decrease as a consequence of deposition and radioactive decay.

## 3. Calculation of concentration

Historically, the calculation of concentration at a receptor in Lagrangian particle models has been made by the *box counting* technique, i.e. by counting the number of particles within a “box” that is centered on the receptor and then dividing the total mass of the particles by the box volume. Clearly, this choice requires a large number of particles to obtain an acceptable resolution in the computed concentration field, as well as a dimension of the counting boxes that is large enough to include a statistically significant number of particles so that the computed field is continuous, but not too large so that the concentration field is over smoothed. This large size of the counting boxes also reduces the vertical resolution of the computed concentration field. The concentration field computed with the box counting technique is thus

grid-dependent. Even with today calculation resources, the calculation of concentrations with the counting method may be time-consuming.

A different numeric technique for computing concentrations in a Lagrangian particle model is the *kernel density estimator*, which permits a reduction in the number of particles and a computation of a completely grid-free and continuous concentration field in each point of the domain. First examples of kernel application in Lagrangian dispersion models are in Lorimer (1986) and Lorimer and Ross (1986). The kernel method generally uses the particles' position to estimate the so-called bandwidths that act as smoothing parameters.

LAPMOD contains several algorithms for calculating the concentrations, for example the *parabolic kernel* (Uliasz, 1994).

A general formulation for calculating instantaneous concentrations with a kernel is (Uliasz, 1994):

$$C_{IST}(x, y, z) = \sum_{i=1}^N \frac{Q_i}{h_{xi}h_{yi}h_{zi}} K(r_x, r_y, r_z)$$

where:

- N is the number of computational particles that contribute to concentration in the point of interest,
- $Q_i$  is the mass associated to the  $i$ -th computational particle,
- $h_{xi}$ ,  $h_{yi}$  and  $h_{zi}$  are the bandwidths of  $i$ -th particle in the three directions. The bandwidths define the degree of smoothing of the concentration field and depend on particle age.

For the parabolic kernel the K function is defined as:

$$K(r_x, r_y, r_z) = \frac{15}{8\pi} (1 - r^2) I$$

where  $I = 1$  if  $r^2 = r_x^2 + r_y^2 + r_z^2 < 1$ , and  $I = 0$  otherwise.

The bandwidths along x and y directions ( $h_x = h_y$ ) are computed as in Stohl et al. (1998):

$$h_x = A + Bt + C\sqrt{t}$$

where  $t$  is the particle age (s) and A, B and C are coefficients. The bandwidth along z ( $h_z$ ) is computed with the same expression, with  $B = 0$ . It is observed that when the bandwidths are proportional to the age of the particle LAPMOD behaves as a hybrid particle-puff model (Zannetti, 1990).

A discussion about the performance of different kernel density estimators can be found in Vitali et al. (2006).

Another approach consists in estimating the bandwidth via their physical interpretation. For example, Yamada et al. (1987) used a Gaussian kernel estimator where the bandwidths are determined as the time integration of the velocity variances encountered by the particle during its life. This kind of *kernel smoother* (e.g., Hastie et al., 2013) is a statistical non-parametric method that allows for making an estimate in a *query point* (a receptor, in our case) of a multidimensional function (the concentration field) through the knowledge of a limited number of observations (the concentration associated to the mass represented by the particle). By using only local observations the resulting estimate is smooth. Localization is obtained by considering only a limited number of observations that are close in space and are weighted based on their distance from the query point. Following this approach, in LAPMOD we assume that the mass attributed to each particle is distributed in space into an ellipsoid that has a time-growing size whose increments depend on the local diffusion properties of the atmosphere that are experienced by the particle

along its motion. The incremental dimensions are computed at each time step as suggested by Hanna et al. (1982):

$$\begin{cases} \sigma_x^2 = \sigma_y^2 = \sigma_z^2 = \varepsilon t^3 & \text{age} \leq 10^4 \text{ s} \\ \sigma_x = \sigma_y = \sigma_z = 100 t & \text{age} > 10^4 \text{ s} \end{cases}$$

(note that  $\sigma_z$  is limited to  $\sigma_z \leq 0.3 z_i$ ).

We then define the concentration associated to the p-th particle as:

$$c_p = \frac{m_p}{\frac{4}{3} \pi \sigma_{xp} \sigma_{yp} \sigma_{zp}}$$

and the kernel smoothing function associated to the particle in the query point  $(x_0, y_0, z_0)$  as:

$$K_p(x_0, y_0, z_0) = \begin{cases} \left(1 - \frac{|x_p - x_0|}{\alpha \sigma_{xp}}\right) \left(1 - \frac{|y_p - y_0|}{\alpha \sigma_{yp}}\right) \left(1 - \frac{|z_p - z_0|}{\alpha \sigma_{zp}}\right) & \text{where } |w_p - w_0| \leq \alpha \sigma_{wp} \quad \forall w \in \{x, y, z\} \\ 0 & \text{elsewhere} \end{cases}$$

$\alpha$  is the “search radius” in  $\sigma$  units. Where the particles’ density is higher,  $\alpha$  must be smaller to guarantee appropriate localization. Since particles released from a source separate each other with time, we assume in LAPMOD that the  $\alpha$  parameters for each particle depend from particle age, up to a limit value.

The general expression for  $\alpha$  is thus:

$$\alpha(t) = \begin{cases} \left(1 + \beta \frac{\text{age}(t)_p}{\text{AGE}}\right) & \text{if } t \leq \text{AGE} \\ \alpha_{\text{max}} & \text{otherwise} \end{cases}$$

The selected default values for LAPMOD are AGE = 1200 s and  $\beta = 1$  (i.e.  $\alpha_{\text{MAX}} = 2$ ).

The concentration in  $(x_0, y_0, z_0)$  is then:

$$C(x_0, y_0, z_0) = \sum_p c_p K_p(x_0, y_0, z_0)$$

#### 4. LAPMOD modeling system structure

The LAPMOD modeling system structure is schematically represented in Fig. 1. The meteorological input of LAPMOD consists of three dimensional fields of wind and temperature, and two dimensional fields of atmospheric turbulence parameters (Monin Obukhov length, friction velocity, convective scale velocity, mixing height). All these input variables are read directly from the CALMET (Scire et al., 1999a) output file. CALMET is the diagnostic meteorological model that prepares input data for the CALPUFF dispersion model (Scire et al., 1999b), which is on the list of the US-EPA preferred/recommended models. The geophysical variables needed by LAPMOD (e.g., the roughness length or the land use category needed for estimating deposition fluxes) are also read from the CALMET output file.

The LAPMOD meteorological input file can also be prepared with the LAPMET processor which reads the surface and profile meteorological files of AERMOD (EPA, 2004), also on the list of the US-EPA preferred/recommended models, and creates an output file formatted as the CALMET output file. The wind and temperature fields prepared by LAPMET are horizontally homogeneous but vary along the vertical direction. The use of the LAPMET processor is useful for simple applications, when the meteorological fields and stations needed by CALMET are not available, and for validation purposes since the meteorological input file of AERMOD is often provided.

The LAPEMI processor produces the LAPMOD emission file with 1-h time resolution starting from the annual average emission of each single source and using three temporal modulation profiles: an annual profile composed by 12 numbers (one for each month), a weekly profile composed by seven numbers (one for each day), and a daily profile composed by 24 numbers (one for each hour). Different sources can share the same profiles if they have similar time variations. LAPEMI is useful for processing emissions for permit applications; however, LAPMOD is capable of managing the emission variations up to the time resolution of 1 s. Time resolutions of minutes or less are typical in accidental releases and in odor modeling.

LAPMOD can be used in two different ways when simulating odor emissions: 1) by calculating the 1-h average concentrations and then applying a peak-to-mean ratio (PMR) for estimating averages over shorter time periods (e.g. 1 or 5 min); or 2) storing for each hour the highest concentration value estimated during each short sampling (i.e. few minutes) carried out for calculating the 1-h average. The peak-to-mean ratio for calculating peak odor concentrations from the 1-h averages is often a constant determined with the Smith (1973) relation (e.g., a value of 2.3). The adoption of this constant is a simplification because the peak concentration varies with atmospheric stability and is not always proportional to the 1-h average concentration with the same constant factor. LAPMOD contains a routine for calculating peak concentrations as described by Mylne (1990, 1992). The same approach is also implemented in the AODM model (Schauburger et al., 2000).

LAPOST is the post processor which reads the LAPMOD binary output file, containing for example the hourly concentration results

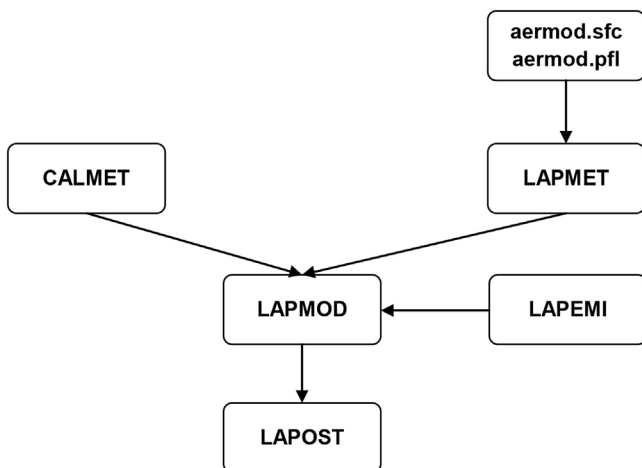


Fig. 1. LAPMOD model system structure.

for one year, and calculates the statistics required by the user (e.g., annual average, 1-h maximum with position and date, 24 h maximum, percentiles of different averages, 8-h running average, etc.). In odor modeling LAPOST calculates also the FIDOL parameters (frequency, intensity, duration, offensiveness, and location), with the exception of the odor offensiveness that is a qualitative, human-sensation parameter. LAPOST is also used to extract information about deposition or particles from the unformatted output files.

The running speed of LAPMOD is comparable to the one of CALPUFF and so it can be used for operational short-term applications and air quality assessments over one or more simulation years.

## 5. Evaluation against field data

LAPMOD has been evaluated using the results of the Kincaid field experiments, both considering the short-term releases of SF<sub>6</sub> and the long-term releases of SO<sub>2</sub>. The Kincaid experiment has been widely used to evaluate air dispersion models (e.g. Hurley et al., 2005).

A series of Perl programs have been developed in order to: 1) read the AERMOD input files distributed by the US-EPA; 2) automatically write all the input files needed by LAPMET and LAPMOD; and 3) write the batch files running the simulations. The files were then checked to look for possible inconsistencies. The SF<sub>6</sub> releases have been managed automatically by means of these programs, while the SO<sub>2</sub> releases required more manual work.

For both the experiments, the CALMET-like meteorological input files have been built with the LAPMET preprocessor starting from the AERMOD meteorological input files distributed by the US-EPA in the model evaluation databases.<sup>1</sup> Meteorology is therefore horizontally homogeneous, but varies along the vertical direction, where the faces of the nine grids were set at the following heights above the ground (in meters): 20, 40, 60, 140, 200, 500, 1000, 2000 and 3000.

The plume rise has been simulated with the algorithm of Webster and Thomson (2002) with  $\alpha_1 = 0.110$ ,  $\alpha_2 = 0.500$ ,  $\alpha_3 = 0.655$  and  $c_D = 0.210$ . For all the evaluations, discrete receptors have been placed exactly at the point where the ambient monitoring stations were located. Among the methods for calculating the concentrations, the Uliasz parabolic kernel has been chosen for this evaluation. The comparisons described below have been carried out with LAPMOD version 2017-05-04.

### 5.1. Kincaid SF<sub>6</sub>

The Kincaid field experiment was performed as part of the EPRI Plume Model Validation and Development Project in 1980 and 1981 (Bowne et al., 1983). The Kincaid power plant is situated in Illinois, USA, and is surrounded by flat farmland and some lakes. The elevation of the ground above sea level is about 180 m, and the roughness length is approximately 0.1 m (Olesen, 2005). The power plant has a 187 m stack with an exit diameter of 9 m. The monitors were placed at ground level at distances ranging from 500 m to 50 km. The meteorological conditions were mostly convective, with some cases of neutral conditions observed.

A quality indicator with values from 0 (worst quality) to 3 (best quality) has been assigned to the observations of Kincaid SF<sub>6</sub>. Only observations of quality 3 have been used for comparison with the model predictions. The comparison has been made with the Model

Validation Kit (Olesen, 2005), hereafter referred to as MVK.

The statistical tool distributed with the MVK requires the normalization of the predicted concentrations, and of the observations, with the release rate. However, LAPMOD is a 3D non-stationary dispersion model; therefore, contrary to the Gaussian plume stationary model in which the plume is immediately present at all downwind receptors, some time is needed for the plume to travel before impacting the receptors downwind. Concentration is different from zero at a given receptor up to the moment that at least one computational particle gets close enough to it, so that the receptor is within the field of the particle's kernel (i.e. of its mass distribution). The normalization of the concentration values with the emission rate, as pointed out by Webster and Thomson (2002), is more meaningful for stationary models because far from the source (Kincaid has receptors up to 50 km from the source) the maximum concentration can be predicted at a time characterized by an emission rate different from the one which caused the maximum. For this reason, the model results and the observations were normalized only when the MVK was applied to compare the results of LAPMOD to those of other models. Where not explicitly indicated, predicted and observed concentrations are not normalized and therefore expressed in  $\mu\text{g}/\text{m}^3$ .

The scatter plot of predictions against observations, both in  $\mu\text{g}/\text{m}^3$ , is shown in Fig. 2, left. The region of FA2 (59.5%) is delimited by two solid lines starting from the origin, while the region of FA5 (85.5%) is delimited by two dashed lines. In general, FA $\alpha$  indicates the percent of data which satisfies  $1/\alpha \leq C_p/C_o \leq \alpha$ , where  $C_p$  is the prediction and  $C_o$  the observation.

The Q-Q plot (Fig. 2, right) represents observations and predictions separately ranked, and it is useful to see whether their cumulative distribution functions (CDFs) are similar. It is observed that LAPMOD has a slight tendency to underpredict for small values of concentrations (up to about 1.4  $\mu\text{g}/\text{m}^3$ ).

The residual box plots for Kincaid quality 3 data are reported in Fig. 3. It is observed that the data sum to 324, while quality 3 data are 338, because there are 14 situations where LAPMOD does not predict any concentration. The residuals are shown as a function of the time of day (Hour; a surrogate for solar radiation), the friction velocity ( $U^*$ ; indicator of wind speed), the mixing height ( $Z_i$ ), and the stability parameter ( $Z_i/L$ ; ratio between mixing height and Monin Obukhov length). The residuals have been grouped according to classes of the above variables, for each class they have been ranked and represented. The lower and upper whiskers represent the 5th and the 95th percentiles respectively, the lower and the upper part of the gray boxes represent the 25th and the 75th percentile respectively, and the thick black horizontal segment represent the median (i.e. 50th percentile) of the distribution. The horizontal lines represent the FA2 area. The ratio between predictions and observations for a perfect model should always be 1.

The LAPMOD results show that the medians of the ratios are almost always close to 1, and a significant proportion of the residuals falls between a factor of 2.

The LAPMOD results have been compared against those of other dispersion models using the Model Validation Kit (Olesen, 2005). Table 1 shows the performances of LAPMOD and those of other dispersion models against the measurements carried out at Kincaid. The other models considered are HPDM (Earth Tech, USA), OML (NERI, Denmark), ADMS 3 (CERC, UK), AERMOD (EPA, USA), ISCST3 (EPA, USA) and NAME (Met Office, UK). Excluding LAPMOD, the data in Table 1 have been taken from Webster and Thomson (2002). Only the Kincaid observations characterized by a quality indicator equal to 3 have been considered, for a total of 338 data. Both observations and model predictions have been normalized by dividing the concentrations for the emission rate and multiplying

<sup>1</sup> [https://www3.epa.gov/ttn/scram/dispersion\\_prefrec.htm](https://www3.epa.gov/ttn/scram/dispersion_prefrec.htm) (Visited on May 17, 2017).

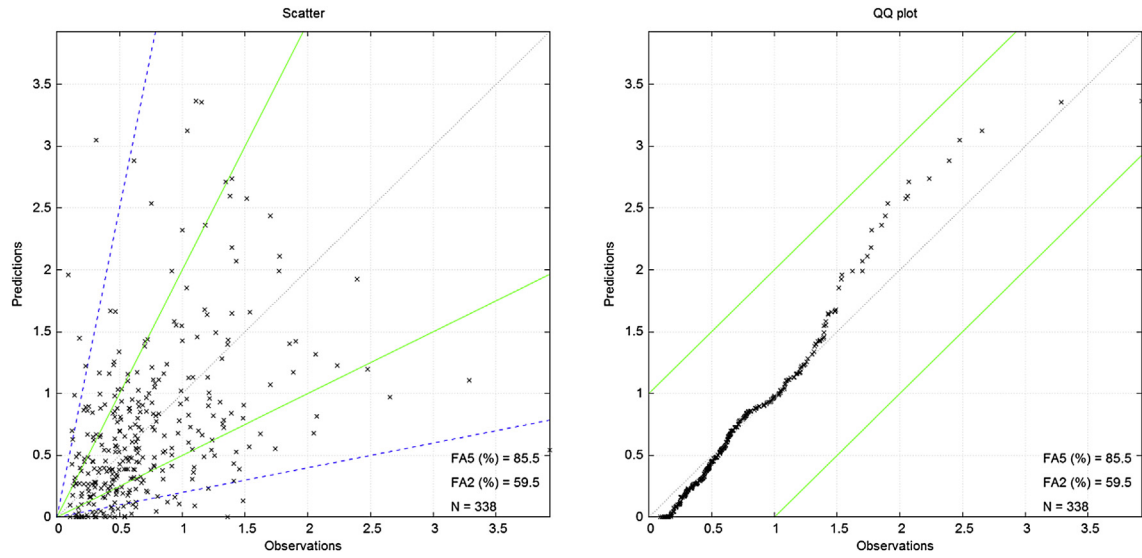


Fig. 2. Scatter plot (left) and QQ plot (right) for Kincaid quality 3 data.

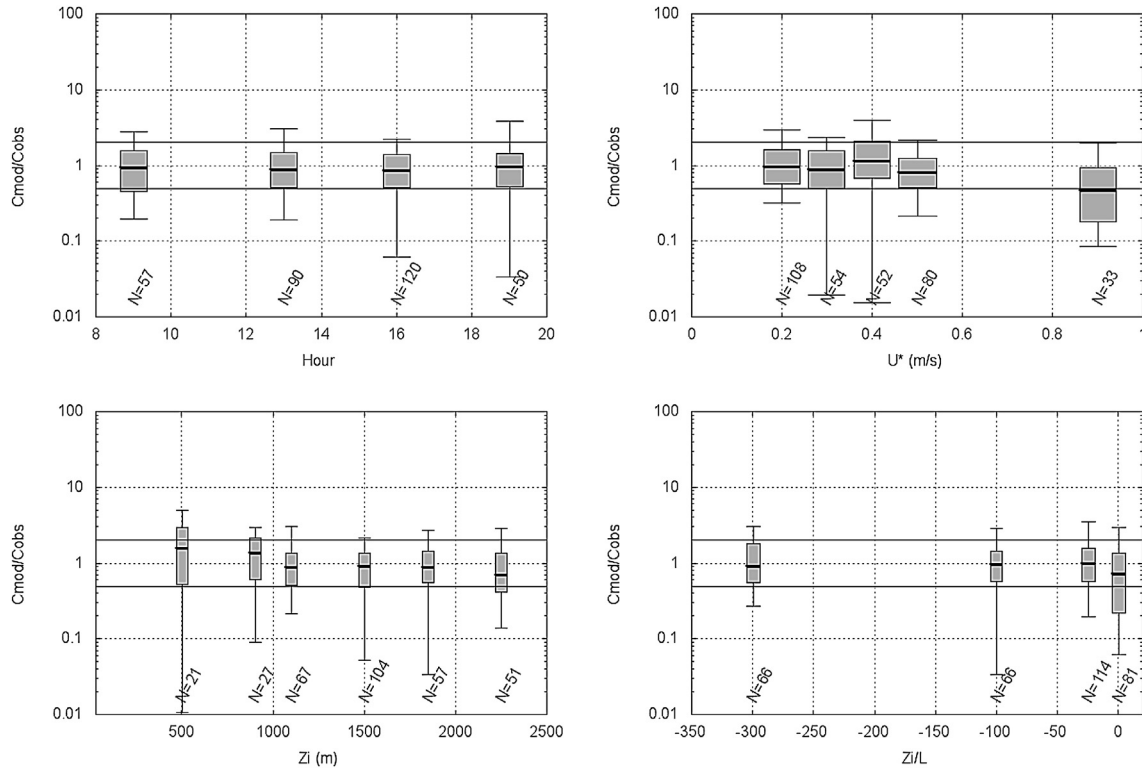


Fig. 3. Residual box plot for Kincaid quality 3 data.

by one thousand. The FS parameter is calculated as  $FS = 2 * (\sigma_{Obs} - \sigma_{Mod}) / (\sigma_{Obs} + \sigma_{Mod})$ .

Other LAPMOD statistics, not reported in Table 1, are (all significantly different from zero at 95% confidence limits):  $FBfn = 0.312$ ,  $FBfp = 0.289$ ,  $MOEfn = 0.692$  and  $MOEfp = 0.708$ . The FB parameter for LAPMOD ( $FB = FBfn - FBfp$ ) is not significantly different from zero at 95% confidence limits. The first maximum predicted by LAPMOD is 272.70 (observed: 319.30), and the second maximum is 268.20 (observed: 225.10).

Chang and Hanna (2004, 2005) propose some performance

evaluation criteria to define a “good” model. They require that at the same time the following three rules be observed:

- the fraction of predictions within a factor of two of observations is about 50% or greater (i.e.,  $FA2 > 50\%$ );
- the mean bias is within  $\pm 30\%$  of the mean (i.e., roughly  $|FB| < 0.3$  or  $0.7 < MG < 1.3$ );
- the random scatter is about a factor of two to three of the mean (i.e., roughly  $NMSE < 1.5$  or  $VG < 4$ ).

**Table 1**  
Performance statistics of some dispersion models for the Kincaid observations of quality 3.

Model	Mean	$\sigma$	Bias	NMSE	r	FB	FS	FA2
Observations	54.34	40.25	0.00	0.00	1.000	0.000	0.000	1.000
LAPMOD	53.11	48.02	1.23	0.76	0.448	0.023	-0.176	0.595
HPDM	44.84	38.55	9.50	0.75	0.441	0.192	0.043	0.565
OML	47.45	45.48	6.89	1.24	0.146	0.135	-0.122	0.547
ADMS 3	51.7	34.7	2.7	0.6	0.45	0.05	0.15	0.67
AERMOD	21.8	21.8	32.6	2.1	0.40	0.86	0.59	0.29
ISCST3	30.0	60.0	24.3	2.8	0.26	0.58	-0.39	0.28
NAME	40.6	40.4	13.8	1.15	0.279	0.290	-0.005	0.615

**Table 2**  
Extreme statistics for the Kincaid quality 3 observations. Values for the NAME model are taken from Webster and Thomson (2002).

Extreme statistics	Observations	LAPMOD	NAME
Maximum concentration	3.928	3.367	3.929
Top ten average	2.506	2.894	2.919
RHC <sub>11</sub>	3.606	3.707	4.328

As recognized by Chang and Hanna (2004), the above rules are not firm guidelines and it is necessary to consider all performance measures in making a decision concerning model acceptance. LAPMOD satisfies the three rules in this case study.

The robust higher concentration, RHC<sub>R</sub> (Cox and Tikvart, 1990), is a good statistical indicator for judging the ability of a model to represent the extreme concentration values. It is calculated as

$$RHC_R = C_R + (C_M - C_R) \ln\left(\frac{3R - 1}{2}\right)$$

where C<sub>R</sub> is the R<sup>th</sup> highest concentration and C<sub>M</sub> is the average of the R-1 highest values. The calculation of RHC<sub>R</sub>, with R = 11, gives the results shown in Table 2. The statistics are reported for the observations, for LAPMOD and, for comparison purposes, for the NAME model (Webster and Thomson, 2002). Apart from the maximum concentration, which is perfectly matched by NAME, the top ten average and the RHC<sub>11</sub> calculated by LAPMOD are similar to observations, with a slight tendency for LAPMOD to underestimate.

5.2. Kincaid SO<sub>2</sub>

The Kincaid SO<sub>2</sub> study (Bowne et al., 1983; Liu and Moore, 1984) was conducted at the same location as the Kincaid SF<sub>6</sub> study. It involved a buoyant, continuous release of SO<sub>2</sub> from a 187 m stack in rural flat terrain. The study included about six months of data between April 1980 and June 1981 (a total of 4614 h of samples). There were 30 SO<sub>2</sub> monitoring stations providing 1-h averaged samples from about 2 km to 20 km downwind of the stack. Two of the monitoring stations (identified as stations 4 and 8) have been removed from this analysis due to suspicious data (see the US-EPA's model evaluation databases). The positions of source and monitoring stations are illustrated in Fig. 4; the wind rose represented in the same figure shows that the receptors north from the source are often downwind, while in few occasions the plume hits receptors 5 to 10. The Kincaid SO<sub>2</sub> tracer release represents a long term continuous study with no building wake (Perry et al., 2005).

For this long term experiment the comparison has been performed for concentrations paired in time, therefore it is more demanding than the previous comparison (Kincaid SF<sub>6</sub>) that was based on the maximum concentrations observed or predicted over an arc.

In the US-EPA's AERMET output file for Kincaid SO<sub>2</sub> the

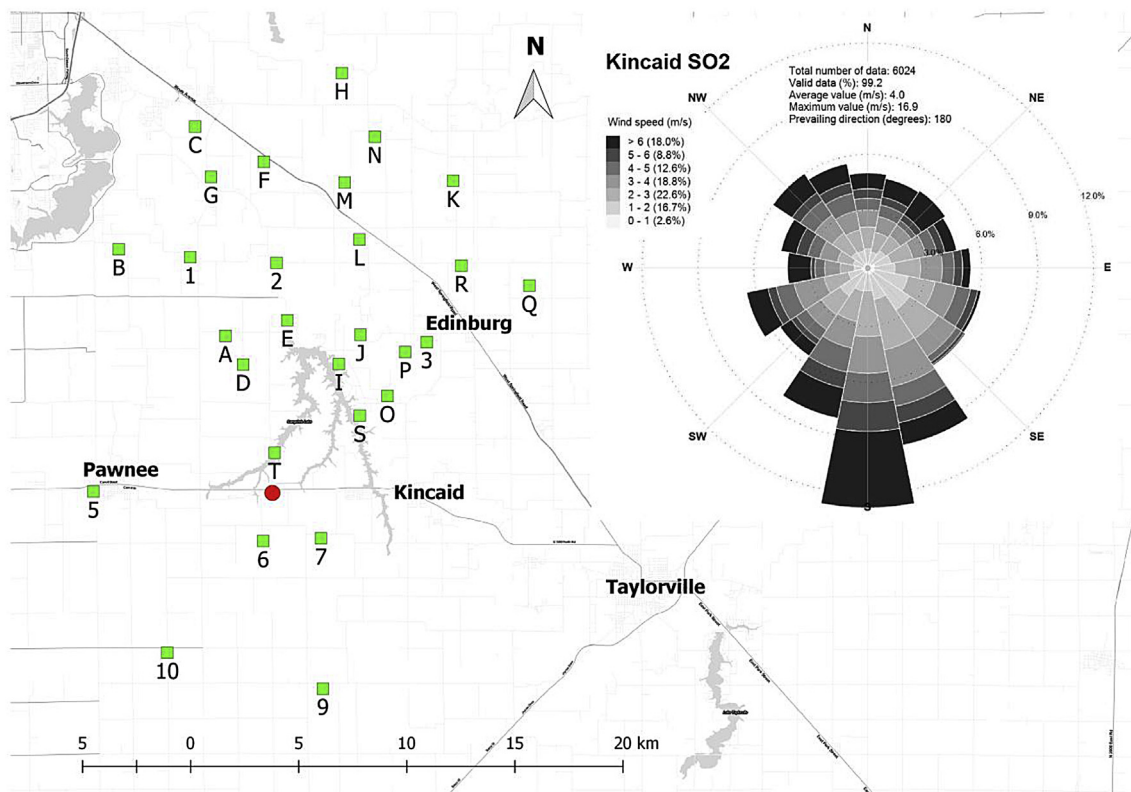


Fig. 4. Source (circle) and monitoring positions (squares) in Kincaid SO<sub>2</sub>. The wind rose is obtained from the AERMET surface meteorological input file.

temperature at hour 9 p.m. of April 17 1980 is 247 K. It has been substituted with 284.6 K, which is the average value of hours 8 p.m. (285.4 K) and 10 p.m. (283.9 K). It is also observed that, in some hours when the convective mixing height is not valid, the mechanical mixing height is 5 m or 10 m, which are very low values that might indicate a ground based inversion.

Some SO<sub>2</sub> observations are non-zero when the SO<sub>2</sub> emissions from the stack are zero. These non-null values while the stack is not emitting are probably due to other sources in the Kincaid area plus background. The predictions of AERMOD and LAPMOD are correctly zero when the emissions are zero. The hours with null emissions have been discarded before performing the model evaluation.

The QQ plot obtained for the 1-h average SO<sub>2</sub> concentration is shown in Fig. 5 for LAPMOD (left) and AERMOD (right). It is observed that the AERMOD plots reported in this section have been created with the predictions distributed with the model evaluation databases, which refer to a previous version of the model. Both models underestimate the 1-h concentrations; the LAPMOD

concentration distribution is close to the observations one up to about 400 µg/m<sup>3</sup>, while the underestimation is more pronounced for higher values. On the contrary, for higher concentrations the AERMOD predictions are closer to the observations. The AERMOD ability to describe peak concentrations has been described by Perry et al. (2005). The results for robust higher concentration also confirm this ability with RHC<sub>26</sub> equal to 1327.3, 1329.0, and 1021.5 respectively for observations, AERMOD, and LAPMOD. Note that R = 26 has been used here for RHC<sub>R</sub>, as suggested by Cox and Tikvart (1990), while for Kincaid SF<sub>6</sub> it was R = 11 in order to compare the LAPMOD predictions with those reported in Webster and Thomson (2002).

Fig. 5 also reports the FA2 and FA5 values, which are lower than those predicted for the SF<sub>6</sub> release because, as anticipated, the SO<sub>2</sub> release predictions and observations at each receptor have been paired in time. The values of these two statistics are similar for the two models.

The QQ plot obtained for the 24-h average SO<sub>2</sub> concentration is

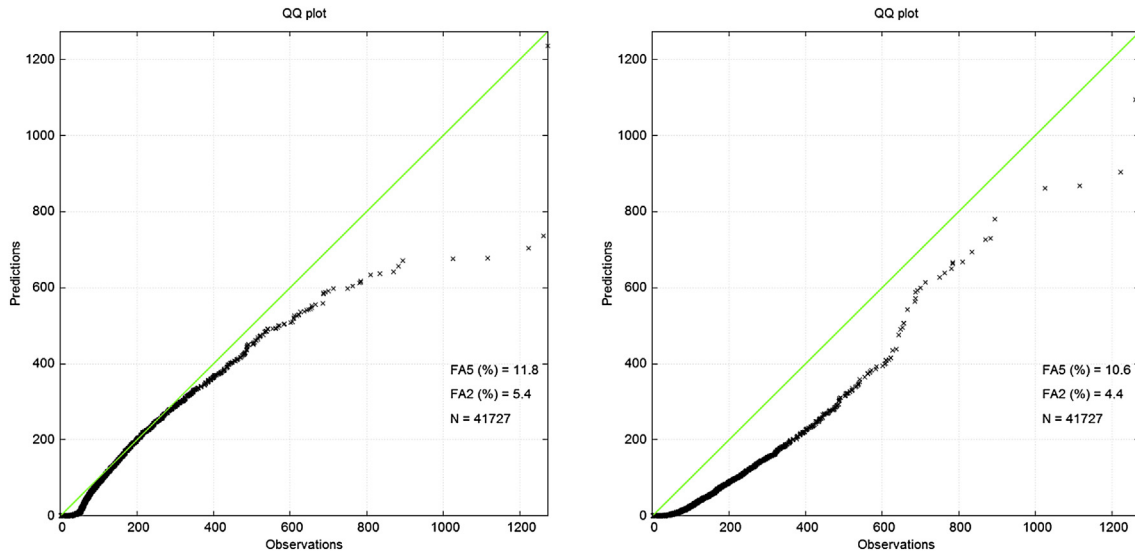


Fig. 5. QQ plot of LAPMOD (left) and AERMOD (right) for 1-h concentrations of Kincaid SO<sub>2</sub>.

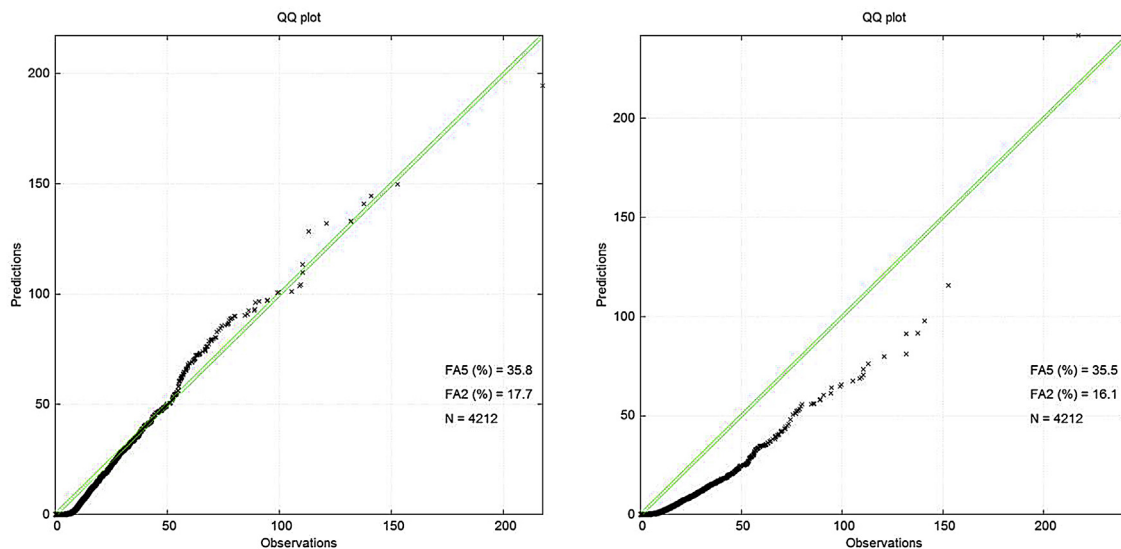


Fig. 6. QQ plot of LAPMOD (left) and AERMOD (right) for 24-h concentrations of Kincaid SO<sub>2</sub>.

shown in Fig. 6 for LAPMOD (left) and AERMOD (right). AERMOD still underestimates the observations, while LAPMOD shows a distribution in good agreement with the measurements.

The period-averaged concentrations at each receptor are shown

in Fig. 7. The LAPMOD average concentrations are in good agreement with the observations, with an FA2 value of 64.3% for LAPMOD and 10.7% for AERMOD.

Finally, the RHC<sub>26</sub> values at each receptor are shown in Fig. 8.

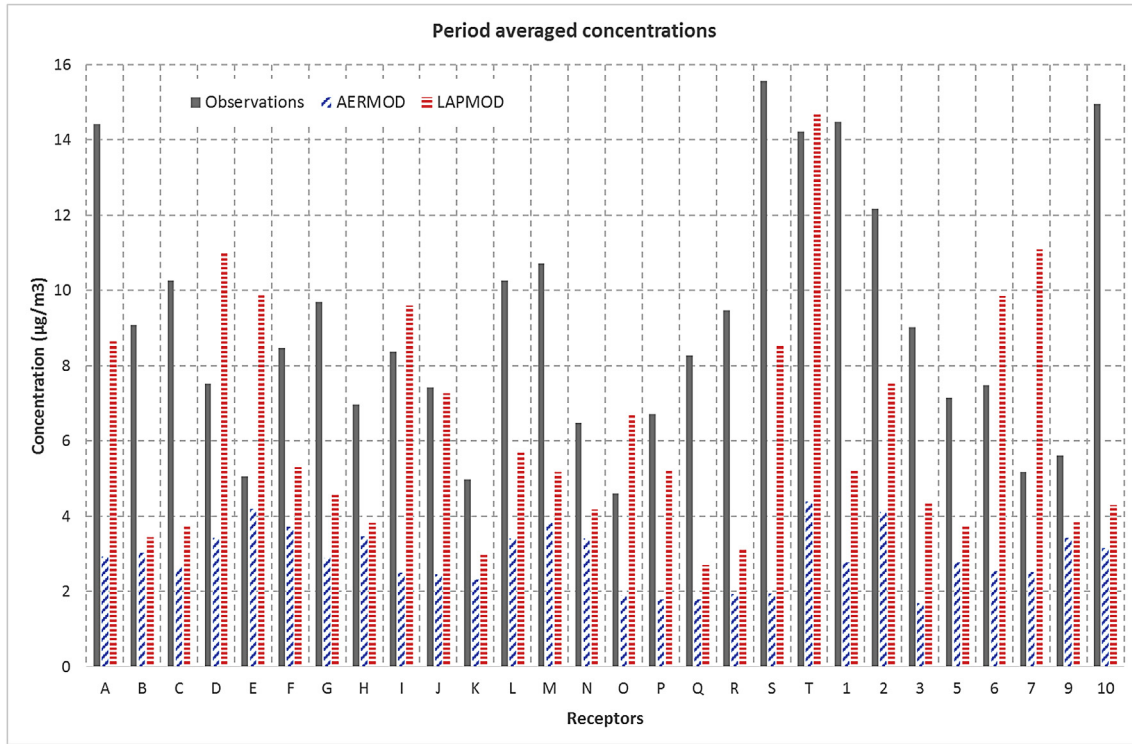


Fig. 7. Period averaged concentrations for observations, AERMOD, and LAPMOD predictions.

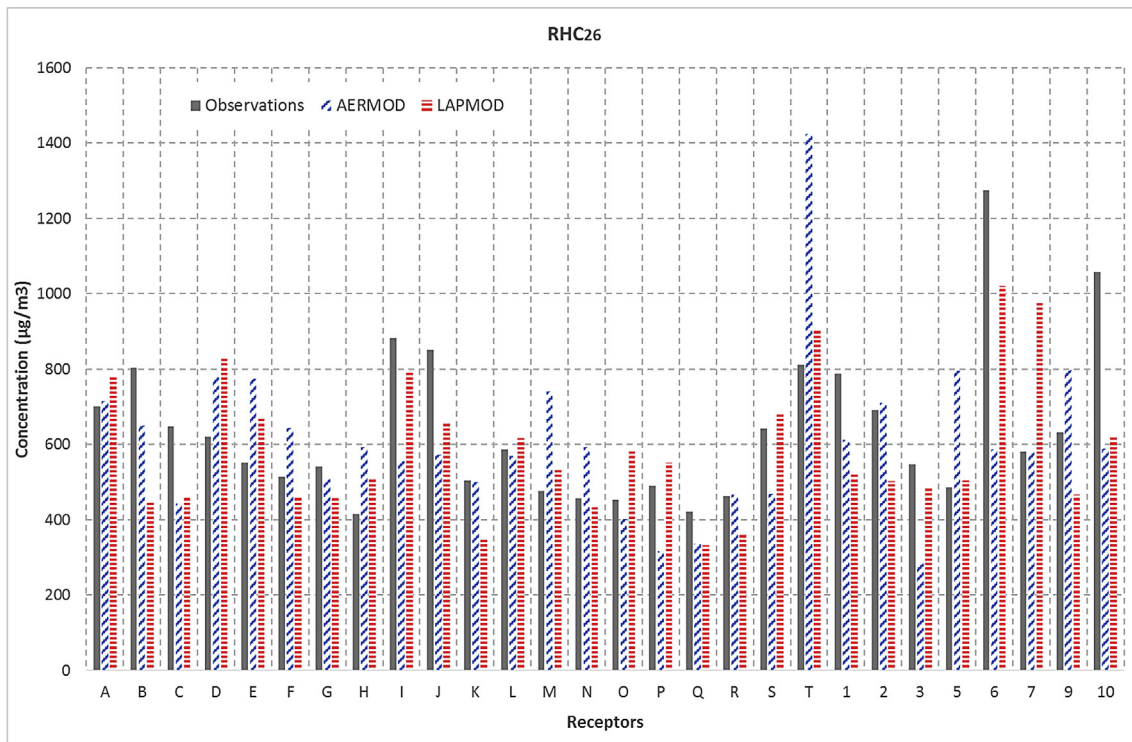


Fig. 8. RHC<sub>26</sub> concentrations for observations, AERMOD, and LAPMOD predictions.

When considering the single receptors, instead of the whole 1-h concentration distribution independently from the position, the ability of LAPMOD to reproduce the peak concentrations appears improved. Considering the ratio between predicted and observed  $RHC_{26}$ , the receptors with such a ratio within the interval [0.85, 1.15] are 28.6% and 39.3% for AERMOD and LAPMOD, respectively.

Fig. 8 shows that the maximum AERMOD  $RHC_{26}$  (about  $1424 \mu\text{g}/\text{m}^3$ ) is predicted at receptor T (the closest to the source at north), where observations and LAPMOD give a value of  $811 \mu\text{g}/\text{m}^3$  and  $904 \mu\text{g}/\text{m}^3$ , respectively. The maximum observed  $RHC_{26}$  is at receptor 6 (the closest to the source at south), where the predicted  $RHC_{26}$  are  $587 \mu\text{g}/\text{m}^3$  and  $1020 \mu\text{g}/\text{m}^3$ , respectively, for AERMOD and LAPMOD. There are also receptors where a good agreement is observed between observations and AERMOD, while LAPMOD overpredicts (e.g., receptor 7).

## 6. Conclusions

This paper describes the theory behind the Lagrangian particle model LAPMOD and all the software processors composing the LAPMOD modeling system. LAPMOD is fully linked to the US-EPA CALMET diagnostic meteorological model and, through its pre-processor LAPMET, to the meteorological files created by AERMET for AERMOD.

The LAPMOD execution times are comparable to those of CALPUFF, and therefore LAPMOD is a cost-effective choice for air quality studies. Moreover, the structure of Lagrangian particle models is such that they can highly benefit from parallelization, for example distributing the particles' movements to different processors. In the future, LAPMOD is expected to implement parallelization and be linked with other software modules simulating atmospheric flows outdoors and indoors.

LAPMOD is capable of simulating emissions with high time resolution and incorporates numerical schemes to treat plume rise and algorithms for estimating peak concentrations that may be also useful for odor studies and accidental releases. Concentrations can be calculated with different kernel methods independently of any grid mesh.

Particle files extracted with the LAPOST processor can be imported in Google Earth and in many GIS systems. Since particles are tagged by their sources, it is possible to track the particles emitted by a specific source and its relative impact. In addition to the emitting source, other parameters such as radioactive decay and deposition can be associated to each particle.

The validation of LAPMOD against the Kincaid data for short term ( $\text{SF}_6$ ) and long term ( $\text{SO}_2$ ) averages has given good results, particularly when compared with the results of other well known models used for regulatory studies.

The LAPMOD system is still under development and testing. The authors are working to introduce building downwash capabilities and to validate the model against other tracer data and model results.

The LAPMOD system is distributed through the Enviroware's web site (<https://www.enviroware.com/lapmod>).

## References

- Armand, P., Brocheton, F., Poulet, D., Vendel, F., Dubourg, V., Yalamas, T., 2014. Probabilistic safety analysis for urgent situations following the accidental release of a pollutant in the atmosphere. *Atmos. Environ.* 96, 1–10. <https://doi.org/10.1016/j.atmosenv.2014.07.022>.
- Baklanov, A., Sorensen, J.H., 2001. Parameterisation of radionuclide deposition in atmospheric Long-Range transport modeling. *Phys. Chem. Earth (B)* 26 (10), 787–799.
- Bellasio, R., Scarpato, S., Bianconi, R., Zeppa, P., 2012. APOLLO2, a new long range Lagrangian particle dispersion model and its evaluation against the first ETEX tracer release. *Atmos. Environ.* 57, 244–256. <https://doi.org/10.1016/j.atmosenv.2012.04.017>.
- Bianconi, R., Mosca, S., Graziani, G., 1999. PDM: a Lagrangian Particle Model for Atmospheric Dispersion. European Commission, p. 63. EUR 17721 EN.
- Bonafè, G., Bianconi, R., Bellasio, R., 2015. The LAPMOD SA modelling system for source attribution. In: 34th International Technical Meeting on Air Pollution Modelling and its Application.
- Bowne, N.E., Londergan, R.J., Murray, D.R., Borenstein, H.S., 1983. Overview, Results, and Conclusions for the EPRI Plume Model Validation and Development Project: Plains Site. EPRI Report EA-3074, Project 1616–1. Electric Power Research Institute, Palo Alto, CA, p. 234.
- Brioude, J., Arnold, D., Stohl, A., Cassiani, M., Morton, D., Seibert, P., Angevine, W., Evan, S., Dingwell, A., Fast, J.D., Easter, R.C., Pizzo, I., Burkhardt, J., Wotawa, G., 2013. The Lagrangian particle dispersion model FLEXPART-WRF version 3.1. *Geosci. Model Dev.* 6, 1889–1904. <http://dx.doi.org/10.5194/gmd-6-1889-2013>.
- Chang, J.C., Hanna, S.R., 2004. Air quality model performance evaluation. *Meteorol. Atmos. Phys.* 87, 167–196.
- Chang, J.C., Hanna, S.R., 2005. Technical Descriptions and User's Guide for the BOOT Statistical Model Evaluation Software Package, Version 2.0. Available at: <http://www.harmo.org/kit/Download.asp> (last visited: May 17, 2017).
- Cox, W.M., Tikvart, J.A., 1990. A statistical procedure for determining the best performing air quality simulation model. *Atmos. Environ.* 24, 2387–2395.
- Du, S., 1997. Universality of the Lagrangian velocity structure function constant (C0) across different kinds of turbulence. *Bound. Layer Meteorol.* 83, 207–219.
- EPA, 2004. AERMOD: Description of Model Formulation. EPA-4543/R-03/004.
- EPA, 2017. <https://www.epa.gov/scram/air-quality-dispersion-modeling-preferred-and-recommended-models> (last visited: May 17, 2017).
- Franzese, P., Luhar, A.K., Borgas, M.S., 1999. An efficient Lagrangian stochastic model of vertical dispersion in the convective boundary layer. *Atmos. Environ.* 33, 2337–2345.
- Hanna, S.R., Paine, R.J., 1989. Hybrid plume dispersion model (HPDM) development and evaluation. *J. Appl. Meteorol.* 28, 206–224.
- Hanna, S.R., Briggs, G.A., Hosker Jr., R.P., 1982. Handbook on Atmospheric Diffusion. Report DOE/TIC-11223. Technical Information Center, U.S. DOE.
- Hanna, S., White, J., Trolier, J., Vernot, R., Brown, M., Gowardhan, A., Kaplan, H., Alexander, Y., Moussafir, J., Wang, Y., 2011. Comparisons of JU2003 observations with four diagnostic urban wind flow and Lagrangian particle dispersion models. *Atmos. Environ.* 45 (24), 4073–4081. <https://doi.org/10.1016/j.atmosenv.2011.03.058>.
- Hastie, T., Tibshirani, R., Friedman, J., 2013. The Elements of Statistical Learning. Data Mining, Inference, and Prediction, second ed. Springer-Verlag, p. 763.
- Hegarty, J., Draxler, R., Stein, A.F., Brioude, J., Mountain, M., Eluszkiewicz, J., Nehrkor, T., Ngan, F., Andrews, A., 2013. Evaluation of Lagrangian particle dispersion models with measurements from controlled tracer releases. *J. Appl. Meteorol. Climatol.* 52, 2623–2637. <http://dx.doi.org/10.1175/JAMC-D-13-0125.1>.
- Hibberd, M.F., Sawford, B.L., 1994. A saline laboratory model of the planetary boundary layer. *Bound. Layer Meteorol.* 67, 229–250.
- Hurley, P.J., Physick, W.L., 1993. A skewed homogeneous Lagrangian particle model for convective conditions. *Atmos. Environ.* 27A, 619–624.
- Hurley, P.J., Physick, W.L., Luhar, A.K., 2005. TAPM: a practical approach to prognostic meteorological and air pollution modelling. *Environ. Model. Softw.* 20 (6), 737–752. <http://dx.doi.org/10.1016/j.envsoft.2004.04.006>.
- Janicke, U., Janicke, L., 2001. A three-dimensional plume rise model for dry and wet plumes. *Atmos. Environ.* 35 (5), 887–890.
- Liu, M.K., Moore, G.E., 1984. Diagnostic Validation of Plume Models at a Plains Site. EPRI Report No. EA-3077, Research Project 1616-9. Electric Power Research Institute, Palo Alto, CA.
- Lorimer, G.S., 1986. A kernel method for air quality modelling-I: mathematical foundation. *Atmos. Environ.* 20, 1447–1452.
- Lorimer, G.S., Ross, D.G., 1986. The kernel method for air quality modelling—II. Comparison with analytic solutions. *Atmos. Environ.* 20, 1773–1780.
- Luhar, A.K., Britter, R., 1989. A random walk model for dispersion in inhomogeneous turbulence in a convective boundary layer. *Atmos. Environ.* 23, 1911–1924.
- Manins, P.C., 1979. Partial penetration of an elevated inversion layer by chimney plumes. *Atmos. Environ.* 13, 733–741.
- Mylne, K.R., 1990. Concentration fluctuation measurements of a tracer plume up to 1 km range in the atmosphere. In: Ninth Symposium on Turbulence and Diffusion. Roskilde, 168–171.
- Mylne, K.R., 1992. Concentration fluctuation measurements in a plume dispersing in a stable surface layer. *Bound. layer Meteorol.* 60, 15–48.
- Olesen, H.R., 2005. User's Guide to the Model Validation Kit. Research Notes from NERI No. 226, p. 2005.
- Park, S.U., Lee, I.H., Ju, J.W., Joo, S.J., 2016. Estimation of radionuclide ( $^{137}\text{Cs}$ ) emission rates from a nuclear power plant accident using the Lagrangian Particle Dispersion Model (LPDM). *J. Environ. Radioact.* 162–163, 258–262. <https://doi.org/10.1016/j.jenvrad.2016.05.033>.
- Perry, S.G., Cimorelli, A.J., Paine, R.J., Brode, R.W., Weil, J.C., Venkatram, A., Wilson, R.B., Lee, R.F., Peters, W.D., 2005. AERMOD: a dispersion model for industrial source applications. Part II: model performance against 17 field study databases. *J. Appl. Meteor.* 44, 694–708.
- Presotto, L., Bellasio, R., Bianconi, R., 2005. Assessment of the visibility impact of a plume emitted by a desulphuration plant. *Atmos. Environ.* 39 (4), 719–737.
- Rakesh, P.T., Venkatesan, R., Hedde, T., Roubin, P., Baskaran, R., Venkatraman, B., 2015. Simulation of radioactive plume gamma dose over a complex terrain using Lagrangian particle dispersion model. *J. Environ. Radioact.* 145, 30–39.

- <https://doi.org/10.1016/j.jenvrad.2015.03.021>.
- Scire, J.S., Robe, F.R., Fernau, M.E., Yamartino, R.J., 1999a. A User's Guide for the CALMET Meteorological Model (Version 5.0). Earth Tech Inc., September 1999.
- Scire, J.S., Strimaitis, D.G., Yamartino, R.J., 1999b. A User's Guide for the CALPUFF Dispersion Model (Version 5.0). Earth Tech Inc., May 1999.
- Seinfeld, J.H., Pandis, S.N., 1998. Atmospheric Chemistry and Physics. From Air Pollution to Climate Change. John Wiley & Sons.
- Schauberger, G., Piringer, M., Pets, E., 2000. Diurnal and annual variation of the sensation distance of odour emitted by livestock buildings calculated by the Austrian odour dispersion model (AODM). *Atmos. Environ.* 34, 4839–4851.
- Smith, M.E., 1973. Recommended Guide for the Prediction of the Dispersion of Airborne Effluents. ASME, New York.
- Stohl, A., Hittenberger, M., Wotawa, G., 1998. Validation of the Lagrangian particle dispersion model FLEXPART against large scale tracer experiment data. *Atmos. Environ.* 32, 4245–4264.
- Thomson, D.J., 1987. Criteria for the selection of stochastic models of particle trajectories in turbulent flows. *J. Fluid Mech.* 180, 529–556.
- Thomson, D.J., Wilson, J.D., 2012. History of Lagrangian stochastic models for turbulent dispersion. Lagrangian modeling of the atmosphere. Geophysical monograph series 200. Am. Geophys. Union. <http://dx.doi.org/10.1029/2012GM001238>.
- Uliasz, M., 1994. Lagrangian particle dispersion modeling in mesoscale applications. In: Zannetti, P. (Ed.), *Environmental Modeling*, vol. II. Computational Mechanics Publications, Southampton, UK.
- Vitali, L., Monforti, F., Bellasio, R., Bianconi, R., Sacchero, V., Mosca, S., Zanini, G., 2006. Validation of a Lagrangian dispersion model implementing different kernel methods for density reconstruction. *Atmos. Environ.* 40, 8020–8033.
- Webster, H.N., Thomson, D.J., 2002. Validation of a Lagrangian model plume rise scheme using the Kincaid data set. *Atmos. Environ.* 36 (32), 5031–5042.
- Weil, J.C., 1990. A diagnosis of the asymmetry in top-down and bottom-up diffusion using a Lagrangian stochastic model. *J. Atmos. Sci.* 47, 501–515.
- Webster, H.N., Thomson, D.J., 2014. The NAME Wet Deposition Scheme. Forecasting Research Technical Report No: 584. <http://www.metoffice.gov.uk/media/pdf/cla/FRTR584.pdf> (visited on December 1st, 2016).
- Wilson, J.D., Legg, B.J., Thomson, D.J., 1983. Calculation of particle trajectories in presence of a gradient in turbulent-velocity variance. *Bound. Layer Meteorol.* 27, 163–169.
- Wilson, J.D., Zhuang, Y., 1989. Restrictions on the time step to be used in stochastic Lagrangian models of turbulent dispersion. *Bound. Layer Meteorol.* 49, 309–316.
- Yamada, T., Bunker, S., Niccum, E., 1987. Simulations of the ASCOT brush creek data by a nested-grid, second moment turbulence closure model and a kernel concentration estimator. In: *Proceedings of AMS Fourth Conference on Mountain Meteorology*, 25–28 August 1987, Seattle, WA.
- Zanini, G., Bellasio, R., Bianconi, R., Delle Monache, L., Lorenzini, R., Mosca, S., Monforti-Ferrario, F., Peverieri, S., Vitali, L., 2002. PLPM (Photochemical Lagrangian Particle Model): Formulation and preliminary Validation. In: *Eight International Conference on Harmonisation within Atmospheric Modelling for Regulatory Purposes*, Sofia (Bulgaria), 14–17 October 2002.
- Zannetti, P., 1990. *Air Pollution Modeling. Theories, Computational Methods and Available Software*. Springer. <http://dx.doi.org/10.1007/978-1-4757-4465-1>.
- Zhang, L., Gong, S., Padro, J., Barrie, L., 2001. A size segregated particle dry deposition scheme for an atmospheric aerosol module. *Atmos. Environ.* 35, 549–560.